Inorganic Chemistry

Article

pubs.acs.org/IC

Photochromic Hybrid Containing *In Situ*-Generated Benzyl Viologen and Novel Trinuclear $[Bi_3Cl_{14}]^{5-}$: Improved Photoresponsive Behavior by the $\pi\cdots\pi$ Interactions and Size Effect of Inorganic Oligomer

Rong-Guang Lin,[†,‡] Gang Xu,[†] Gang Lu,[†] Ming-Sheng Wang,[†] Pei-Xin Li,[†] and Guo-Cong Guo*[,†]

[†]State Key Laboratory of Structural Chemistry, Fujian Institute of Research on the Structure of Matter, Chinese Academy of Sciences, Fuzhou, Fujian 350002, People's Republic of China

[‡]College of Life Sciences, Fujian Agriculture and Forestry University, Fuzhou 350002, People's Republic of China

Supporting Information

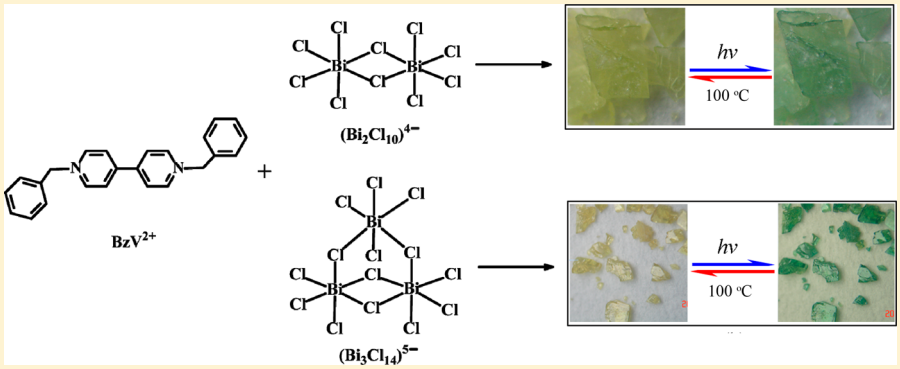

ABSTRACT: Two new member of $(V)_{(2n+2)/2}[Bi_{2n}Cl_{8n+2}]$ series hybrids, $(BzV)_2[Bi_2Cl_{10}]$ (**1**) and $(BzV)_5[Bi_3Cl_{14}]_2\cdot(C_6H_5CH_2)_2O$ (**2**) (where BzV^{2+} = *N*,*N*′-dibenzyl-4,4′-bipyridinium and $(C_6H_5CH_2)_2O$ = dibenzyl ether) have been obtained, and compound **2** contains an unprecedented discrete trimer $[Bi_3Cl_{14}]^{5-}$ counterion. The novel *in situ*-synthesized symmetric viologen cation with aromatic groups on both sides of 4,4′-bipy would provide more opportunities to create $\pi\cdots\pi$ interactions to optimize the photochromic property of the hybrid, and different bismuthated-halide oligomers enable us to discuss the size effect in this series of compounds. Both **1** and **2** are photochromic, and their photoresponsive rate is faster than that of reported viologen−metal halide hybrids. Experimental and theoretical data illustrated that the size of the inorganic oligomer can significantly influence the photoresponsive rate of the viologen dication, and the $\pi\cdots\pi$ interaction behaves as not only a powerful factor to stabilize the viologen monocation radical but also the second electron-transfer pathway, from a π-conjugated substituent to a viologen cation, for the photochromic process.

INTRODUCTION

Inorganic−organic hybrids have been widely studied for several decades, because of the rich diversity of the anionic sublattice and their interesting optical and electric properties,[1] such as semiconductivity, luminescence, and nonlinear optical effect. We and other research groups have witnessed the photochromic properties of viologen bismuthate halides with a common formula of $(V)_{(2n+2)/2}(Bi_{2n}Cl_{8n+2})$ (where V = viologen = *N*,*N*′-disubstituted-4,4′-bipyridinium; n = 0.5, 1, 2, 3, and ∞).[2] The halometalate anion is composed of $BiCl_6$ octahedra, which are able to form either the discrete one-octahedral $[BiCl_6]^{3-}$ (n = 0.5),[3] bioctahedral $[Bi_2Cl_{10}]^{4-}$ (n = 1),[2d,4] four-octahedral $[Bi_4Cl_{18}]^{6-}$ (n = 2),[2c] six-octahedral $[Bi_6Cl_{26}]^{8-}$ (n = 3)[2b,c] units, or the infinite one-dimensional chain $[(Bi_2Cl_8^{2-})_\infty]$ (n = ∞).[2a] The photochromism of viologen bismuthate halides highly depends on the size of the bismuthated-halide oligomer.[2c] Mercier and co-authors found that $(MV)_3[Bi_4Cl_{18}]$ (where MV^{2+} = methyl viologen = *N*,*N*′-dimethyl-4,4′-bipyridinium; n = 2) do not exhibit photochromism, while $(MV)_4[Bi_6Cl_{26}]$ (n = 3) is photochromic active.[2c] However, the influence of trinuclear bismuth (n = 1.5) anions on photochromic effects have not been reported.

On the other hand, the unsymmetrical viologens, which contain a π-conjugated substituent on one side of the 4,4′-bipyridine, can be synthesized *in situ* (Scheme 1), and these show improved photochromic performance, because the $\pi\cdots\pi$ interactions between viologen and phenyl groups act as not

Scheme 1. *In Situ* Syntheses Of Unsymmertical Viologens

R = Benzyl, Phenethyl, Methyl

Received: January 28, 2014
Published: May 20, 2014

   dx.doi.org/10.1021/ic5002144 | *Inorg. Chem.* 2014, 53, 5538−5545

only a powerful factor to stabilize the photogenerated viologen monocation radical but also the second electron-transfer pathway from a π-conjugated substituent to a viologen cation for photochromic process.[2d] It seems reasonable to speculate that the photochromic properties of this series compounds could be further optimized by enriching and enhancing $\pi\cdots\pi$ interactions.

To validate the above hypothesis, extend our *in situ* synthesis to symmetric viologen compound, and also examine the effect of different metal halide counterions on photochromic properties, we have synthesized two new members of the $(V)_{(2n+2)/2}[Bi_{2n}Cl_{8n+2}]$ series hybrid: $(BzV)_2[Bi_2Cl_{10}]$ (**1**) and $(BzV)_5[Bi_3Cl_{14}]_2\cdot(C_6H_5CH_2)_2O$ (**2**) (where BzV^{2+} = *N*,*N*′-dibenzyl-4,4′-bipyridinium; $(C_6H_5CH_2)_2O$ = dibenzyl ether). The novel *in situ*-synthesized symmetric viologen molecule with an aromatic group on both sides of the 4,4′-bipy were designed and synthesized for the first time, which would provide more opportunity to create $\pi\cdots\pi$ interactions to optimize the photochromic property of the hybrid. Meanwhile, different bismuthated-halide oligomer enables us to further reveal the size effect in this field. Herein, we report the syntheses, crystal structures, and the improved photochromic properties of **1** and **2** in this field.

EXPERIMENTAL SECTION

Materials and Methods. $BiCl_3$, 4,4′-bipyridine, benzyl alcohol, and concentrated HCl were used as received. Fourier transform infrared (FT-IR) spectra were recorded in the range 4000−400 cm^{-1} on a Nicolet Model Magna 750 spectrometer using KBr disks. Powder X-ray diffraction (PXRD) patterns were collected with a Rigaku Model MiniFlex2 diffractometer powered at 30 kV and 15 mA for Cu Kα (λ = 1.5406 Å), with a scan rate of 5° min^{-1} at room temperature. Simulated patterns were obtained from the Mercury program using single-crystal reflection diffraction data. EPR studies were conducted on a Bruker Model A300 spectrometer with a 100 kHz magnetic field in the X-band at room temperature. Ultraviolet−visible light (UV-vis) diffuse reflectance spectra were recorded in the wavelength range of 190−820 nm at room temperature on a PE Lambda 900 UV-vis spectrometer equipped with an integrating sphere. A $BaSO_4$ plate was used as a reference (100% reflectance), on which the finely ground powder of the samples were coated. All calculations were performed by using Gaussian 03. The structures of cations were optimized and subsequently characterized by frequency analysis calculations at the B3LYP/6-31G** level.[5] The structures for anions ($[BiCl_6]^{3-}$, $[Bi_2Cl_{10}]^{4-}$, $[Bi_3Cl_{14}]^{5-}$, $[Bi_4Cl_{18}]^{6-}$, and $[Bi_6Cl_{26}]^{8-}$) were taken from those of their crystal geometries and the single-point calculations were carried out using B3LYP functional; the 6-31+G* and LANL2DZ basis sets were used for Cl and Bi, respectively.

Synthesis of 1 and 2. Both **1** and **2** were generated *in situ* under solvothermal conditions from the reaction of $BiCl_3$, concentrated HCl, 4,4′-bipyridine, and benzyl alcohol. The preparation method used here was similar to the synthesis of $(HBzV)_2[Bi_2Cl_{10}]$ (where $HBzV^{2+}$ = *N*-proton-*N*′-benzyl-4,4′-bipyridinium), which contains an unsymmetrically substituted viologen molecule by aromatic group.[2d] However, we found hybrid with symmetric substituted viologen molecule can be synthesized by simply decreasing the volume ratio of concentrated hydrochloric acid to benzyl alcohol from 2:8 for $(HBzV)_2[Bi_2Cl_{10}]$ to 1:9. The reason may be because a lower concentration of hydrochloric acid makes the N atom of 4,4′-bipyridine harder to be protonated and, therefore, easier to be substituted by benzyl.

Compound **1**. $BiCl_3$ (200 mg, 0.63 mmol), 4,4′-bipyridine (90 mg, 0.57 mmol), 1 mL of concentrated HCl (36−38%), and benzyl alcohol (9 mL) were mixed and loaded into a 25-mL Teflon-lined autoclave, which was heated to 140 °C at 2 °C/min and held at that temperature for 2 d, and then cooled to 70 °C at 2 °C/h and held at this temperature for 6 h before cooling to room temperature at the same cooling rate. Platelike yellow single crystals of **1** (45% yield based on $BiCl_3$) was obtained and washed with ethanol. Anal. Calcd (%) for $C_{48}H_{44}Bi_2Cl_{10}N_4$: C 39.89, H 3.07, N 3.88; Found: C 39.77, H 3.04, N 3.93. FT-IR (KBr, cm^{-1}): ν = 3041(s), 1733(m), 1701(m), 1634(s), 1558(s), 1497(m), 1457(s), 1438(s), 1387(w), 1241(w), 1206(m), 1154(w), 1029(w), 809(m), 766(m), 724(s), 701(m), 618(w), 577(w), 556(w) (see Figure S1a in the Supporting Information). The phase purity of the as-synthesized crystalline sample was checked via PXRD (see Figure S2a in the Supporting Information).

Compound **2**. This compound was synthesized according to the same procedure for **1**. The only difference is the amount of 4,4′-bipyridine: 90 mg for **1** and 60 mg for **2**. Blocky yellow single crystals of **2** (70% yield based on $BiCl_3$) was obtained and washed with ethanol. Anal. Calcd (%) for $C_{134}H_{124}Bi_6Cl_{28}N_{10}O$: C 38.90, H 3.02, N 3.39; Found: C 38.78, H 3.24, N 3.36. FT-IR (KBr, cm^{-1}): ν = 3049(s), 1634(s), 1557(m), 1495(m), 1443(s), 1351(w), 1278(w), 1205(w), 1159(m), 1028(w), 850(w), 807(m), 750(s), 700(m), 619(w), 555(w) (see Figure S1b in the Supporting Information). The phase purity of the as-synthesized crystalline sample was checked by PXRD (see Figure S2b in the Supporting Information).

X-ray Crystallographic Study. Single-crystal X-ray diffraction measurements of **1** and **2** were performed on a Rigaku SATURN70 CCD diffractometer, using graphite-monochromated Mo Kα radiation (λ = 0.71073 Å). Intensity datasets were collected using an ω scan technique, and corrected for *Lp* effects. The structures were solved by the direct method using the Siemens SHELXTL Version 5 package of crystallographic software.[6] Difference Fourier maps based on these atomic positions yield other non-hydrogen atoms. The final structures were refined using a full-matrix least-squares refinement on F^2. All non-hydrogen atoms were refined anisotropically. Hydrogen atoms were allowed to ride on their respective parent atoms and included in the structure factor calculations with assigned isotropic thermal parameters. For **2**, one Cl atom in the anion was disordered over three positions, which were refined with an occupancy factor of 0.40/0.30/0.30 for Cl1/Cl1′/Cl1″. Crystal data and structure refinement details for **1** and **2** are summarized in Table 1 and the selected bond lengths and bond angles are given in Table S1 in the Supporting Information.

Table 1. Crystal Data and Structure Refinements for 1 and 2

	1	2
empirical formula	$C_{48}H_{44}Bi_2Cl_{10}N_4$	$C_{134}H_{124}Bi_6Cl_{28}N_{10}O$
formula weight	1449.34	4136.91
color and habit	green block	yellow block
crystal size (mm)	0.37 × 0.16 × 0.10	0.37 × 0.35 × 0.34
crystal system	triclinic	monoclinic
space group	$P\bar{1}$	$P2/c$
a (Å)	10.468(4)	24.430(5)
b (Å)	11.216(4)	12.770(2)
c (Å)	12.826(5)	23.873(5)
α (deg)	77.020(14)	90
β (deg)	80.021(16)	101.738(4)
γ (deg)	64.277(13)	90
V (Å^3)	1317.1(9)	7292(2)
Z	2	2
D_{calcd} (g cm^{-3})	1.827	1.884
μ (mm^{-1})	7.216	7.780
F (000)	696	3960
θ (deg)	3.11−27.45	2.36−25.50
goodness-of-fit on F^2	0.964	1.042
reflections measured	12 726	46 712
number of independent reflections (R_{int})	5752 (0.0345)	13291 (0.0629)
number of observed reflections [$I > 2\sigma(I)$]	5015	11 603
final R_1, wR_2 indices (obs.)	0.0277, 0.0604	0.0518, 0.1108
R_1, wR_2 indices (all)	0.0335, 0.0624	0.0619, 0.1179

dx.doi.org/10.1021/ic5002144 | Inorg. Chem. 2014, 53, 5538−5545

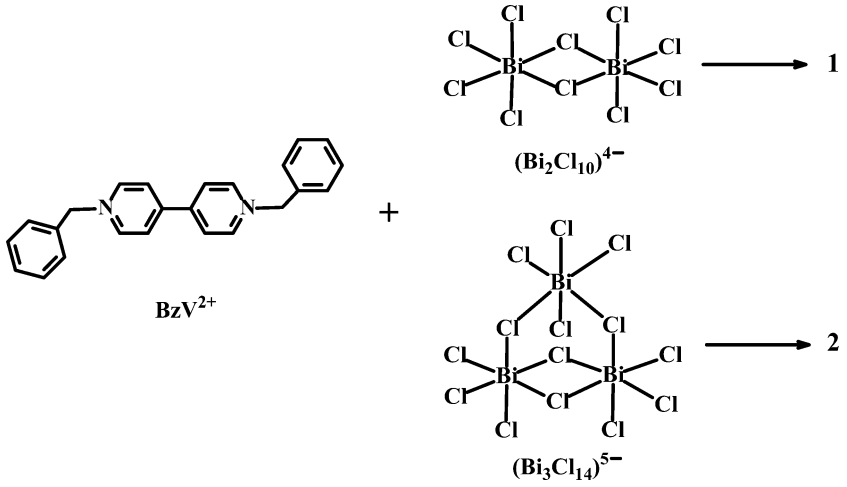

Figure 1. View of the viologen cation and two types of bismuthated-halide anions in **1** and **2**.

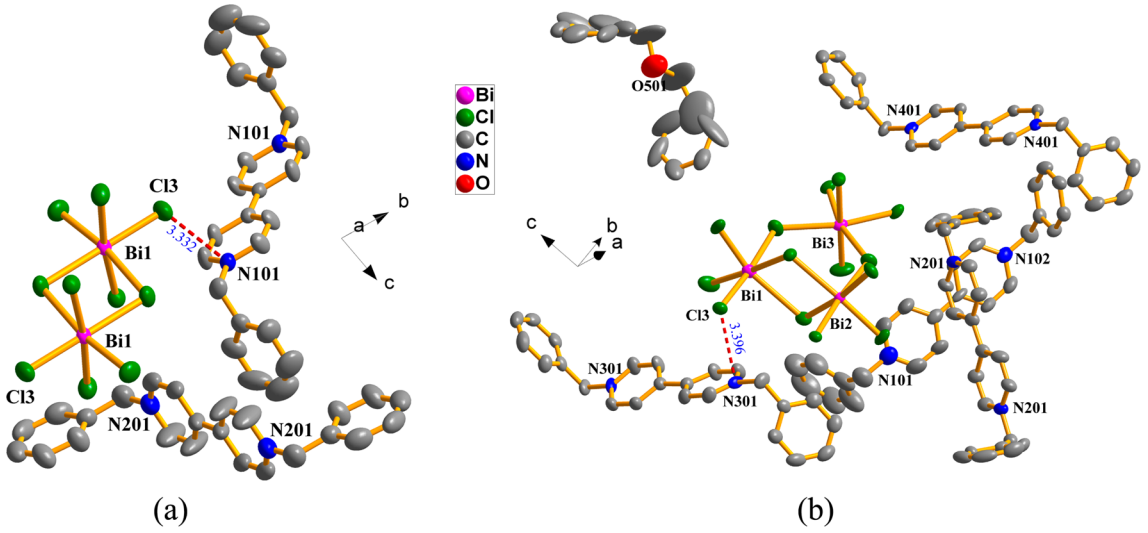

Figure 2. Molecular structures of (a) **1** and (b) **2** (50% thermal probability ellipsoids). The shortest N···Cl distance are displayed by red dotted lines with all hydrogen atoms being omitted for the sake of clarity.

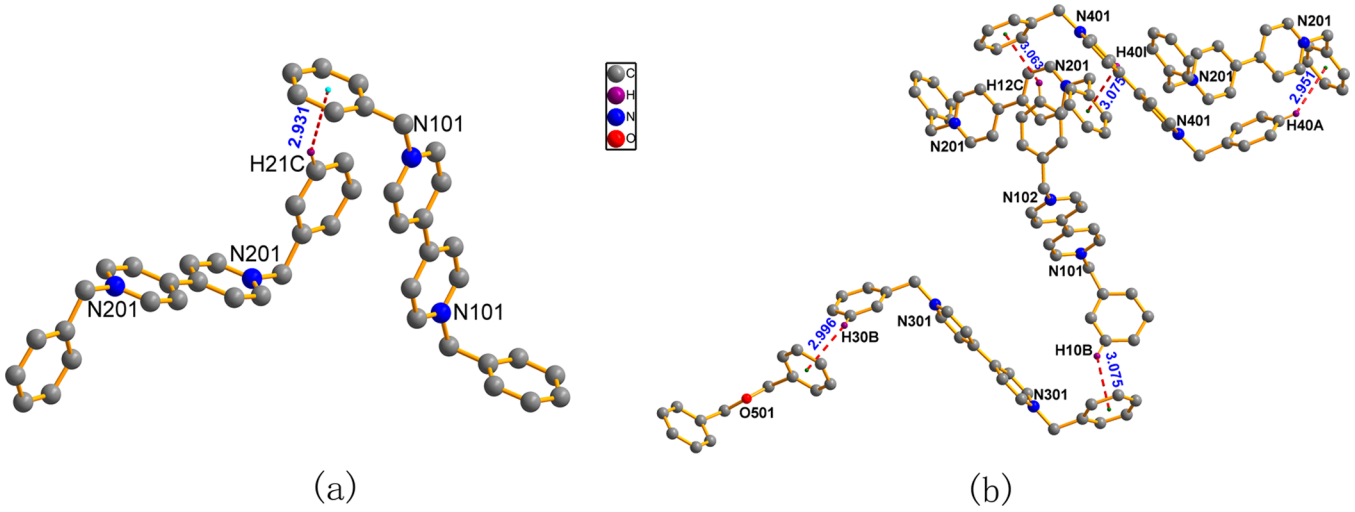

Figure 3. Edge-to-face $\pi\cdots\pi$ interactions (C−H$\cdots\pi$ interactions) in (a) **1** and (b) **2**, which are shown by dashed pink lines. C−H(21C)···Cg(3) = 2.931 Å in **1** and C−H(10B)···Cg(10) = 3.075 Å; C−H(12C)···Cg(11) = 3.063 Å; C−H(30B)···Cg(12) = 2.996 Å; C−H(40A)···Cg(9) = 2.951 Å; C−H(40I)···Cg(9) = 3.075 Å in **2**. Only the hydrogen atoms involved in supramolecular interactions are shown, for the sake of clarity.

dx.doi.org/10.1021/ic5002144 | *Inorg. Chem.* 2014, 53, 5538−5545

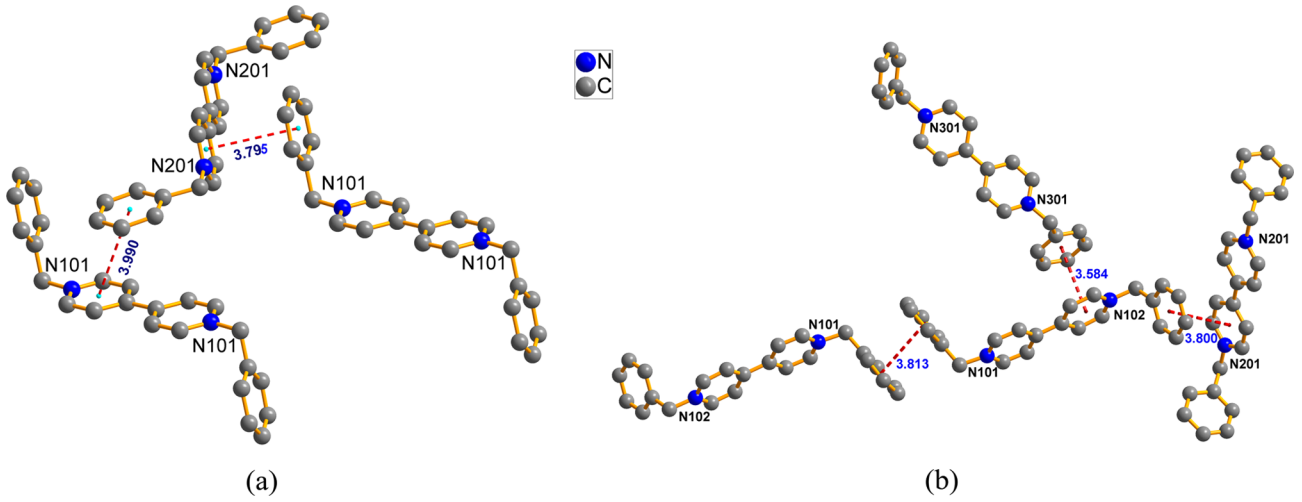

Figure 4. Face-to-face $\pi\cdots\pi$ interactions in (a) **1** and (b) **2** which are shown by dashed pink lines. Cg(2)···Cg(3) = 3.795 Å; Cg(1)···Cg(4) = 3.990 Å in **1** and Cg(5)···Cg(10) = 3.584 Å; Cg(6)···Cg(8) = 3.800 Å; Cg(7)···Cg(7) = 3.813 Å in **2**. All hydrogen atoms are omitted for the sake of clarity.

RESULTS AND DISCUSSION

Description of the Crystal Structures. Compounds **1** and **2** contain the same viologens (BzV^{2+} = *N*,*N*′-dibenzyl-4,4′-bipyridinium) as cations, but different metal halides as anions: $[Bi_2Cl_{10}]^{4-}$ for **1** and $[Bi_3Cl_{14}]^{5-}$ for **2**, respectively (see Figure 1).

Compound **1** crystallizes in the triclinic space group $P\bar{1}$, and its asymmetric unit contains two halves of a BzV^{2+} cation and one half of a $[Bi_2(\mu\text{-}Cl)_2Cl_8]$ anion (Figure 2a). Each $[Bi_2Cl_{10}]^{4-}$ anion consists of two edge-shared $BiCl_6$ octahedra, where the Bi−Cl bonds could be divided into terminal bonds and bridging ones, respectively, with the following bond distances: 2.604(1)−2.710(1) and 2.925(2)−2.936(2) Å. The mean terminal Bi−Cl bond length (2.645 Å) in **1** is almost the same as that of $(HBz)_2[Bi_2Cl_{10}]$ (2.646 Å), while the mean bridging Bi−Cl bond length (2.931 Å) is slightly longer than that of $(HBz)_2[Bi_2Cl_{10}]$ (2.895 Å).[2d] In **1**, the two BzV^{2+} cations are all *trans*−*trans* configurations, and the dihedral angles between the two pyridinium cycles are 0.380° and 0.000°, respectively. The BzV^{2+} cation connect with each other through the edge-to-face C−H···π interactions (see Figure 3a).[7] The distance of C−H···Cg (π−ring) is 2.9308 Å and the angle is 156.82° (see Table S2 in the Supporting Information). Meanwhile, there are also existing face-to-face $\pi\cdots\pi$ interactions between the viologen cations (Figure 4a). The distances between two Cg centroids are 3.795(5) and 3.990(4) Å, and the dihedral angles of those are 9.02° and 8.61°, respectively (see Table S3 in the Supporting Information). The BzV^{2+} cations have appeared in the $(BzV)_2[Bi_2I_8(\mu\text{-}I)_2]$[8] and $[(BzV)_2[Pb_5I_{14}]]_n$[9] compounds, but none of them possess photochromism. As depicted in Figure 2a, the shortest N···Cl distance in **1** belongs to N(101)···Cl(3), with a value of 3.332(4) Å. The angle between the (N101···Cl3) direction and the plane of the pyridinium ring and that of Bi(1)−Cl(3)···N(101) are about 105.76 and 108.90°, respectively. Four BzV^{2+} cations, surrounding each inorganic anion through electrostatic forces, stack along the *a*-axis to yield a channel, where the $[Bi_2Cl_{10}]^{4-}$ anions are encapsulated (see Figure S3a).

Compound **2** crystallizes in the monoclinic space group $P2/c$ and its asymmetric unit comprises one and three halves of a BzV^{2+} cation, one half of a dibenzyl ether molecule, and a $[Bi_3(\mu\text{-}Cl)_4Cl_{10}]^{5-}$ anion (Figure 2b). The $[Bi_3Cl_{14}]^{5-}$ anion may be viewed as the construction of three $BiCl_6$ octahedra bridged by Cl atoms. The three six-coordinate Bi(III) atoms (i.e., Bi1, Bi2, and Bi3) of the anion occupy the vertices of an isosceles triangle. The Bi3 atom bridges Bi1 and Bi2 atoms through μ-Cl9 and μ-Cl14 atoms, respectively, while Bi1 and Bi2 atoms are doubly bridged by μ-Cl4 and μ-Cl8 atoms. The three Bi atoms and the Cl9 and Cl14 atoms locate at the same plane, while the Cl4 and Cl8 atoms form a segment perpendicular to this plane. The $Bi_2(\mu\text{-}Cl)_2$ moiety is also almost planar with a dihedral angle of 177.02° between the (Bi1, Cl4, Cl8) and (Bi2, Cl4, Cl8) planes. The coordination about the unique Bi3 atom is completed by four terminal Cl atoms, while the other Bi atoms (Bi1 and Bi2) have three terminal Cl atoms. There are 10 shorter Bi−$Cl_{terminal}$ bonds (2.525(5)−2.765(1) Å) and eight longer Bi−$Cl_{bridging}$ bonds (2.778(2)−3.176(2) Å) in the $[Bi_3Cl_{14}]^{5-}$. It is worth noting that, although bismuth halide have shown rich structural diversity, such triangle trinuclear bismuth halide described above, to our best knowledge, represents a new type of structural type of bismuth halides. Presently, there are only six types of chlorobismuthate anions have been obtained in viologen chorobismuthate hybrids: one-octahedral $[BiCl_6]^{3-}$,[3] bioctahedral $[Bi_2Cl_{10}]^{4-}$,[2d,4] four-octahedral $[Bi_4Cl_{18}]^{6-}$,[2c] six-octahedral $[Bi_6Cl_{26}]^{8-}$[2b,c] units, or the infinite one-dimensional chain $[(BiCl_5^{2-})_\infty]^4$ and $[(Bi_2Cl_8^{2-})_\infty]$.[2a] Of these siz types of anions, only compounds that contain $[Bi_2Cl_{10}]^{4-}$, $[Bi_6Cl_{26}]^{8-}$, and $[(Bi_2Cl_8^{2-})_\infty]$ inorganic anionic species possess photochromism.[2] Notably, the $[Bi_3Cl_{14}]^{5-}$ anion is unprecedented discrete trimer to viologen chorobismuthate hybrids, and it is crucial to systematically investigate the effect of anion on photochromism. In **2**, the four BzV^{2+} cations are all *trans*−*trans* configurations, and the dihedral angles between the two pyridinium cycles are 3.294°, 0.000°, 19.625°, and 8.213°, respectively. The BzV^{2+} cation connects with other BzV^{2+} cations or dibenzyl ether molecules via C−H···π interactions to form edge-to-face $\pi\cdots\pi$ interactions (Figure 3b). The C···Cg separations for the C−H···Cg (π−ring) interactions are 3.0751, 3.0633, 2.9955, 2.9511, and 3.0753 Å, and the C−H···Cg angles are 140.90°, 145.32°, 142.32°, 139.34°, and 121.03°, respectively (see Table S2 in the Supporting Information). In addition, there are also face-to-face $\pi\cdots\pi$ interactions between the viologen cations (Figure 4b). The distances between two

dx.doi.org/10.1021/ic5002144 | Inorg. Chem. 2014, 53, 5538−5545

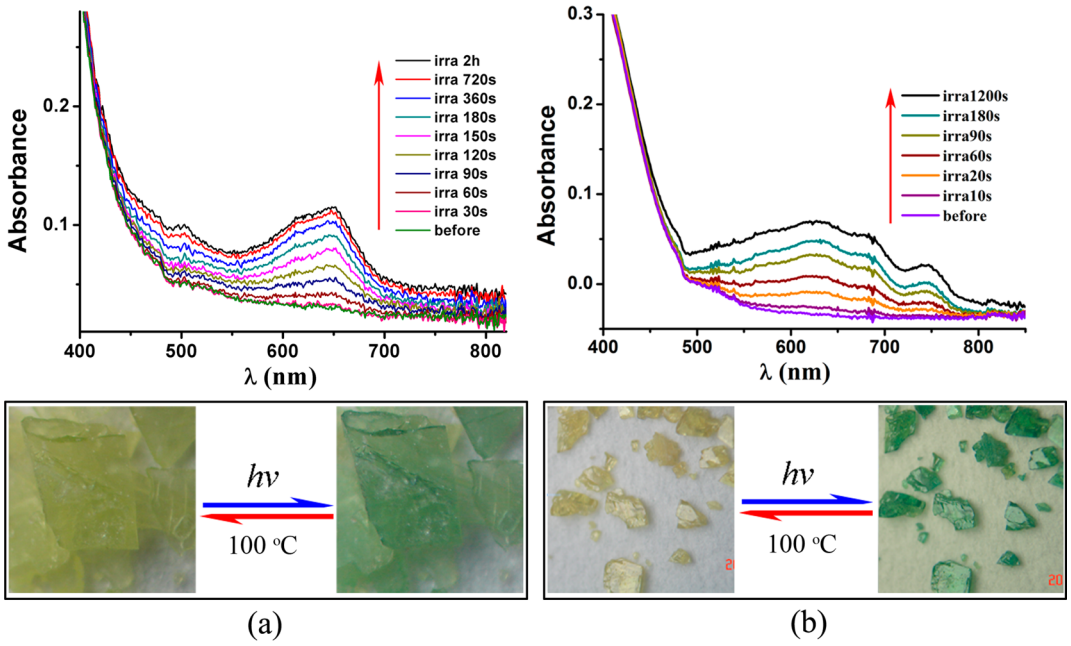

Figure 5. UV−vis diffuse reflectance spectra and photographs showing the photochromic behavior of (a) **1** and (b) **2**.

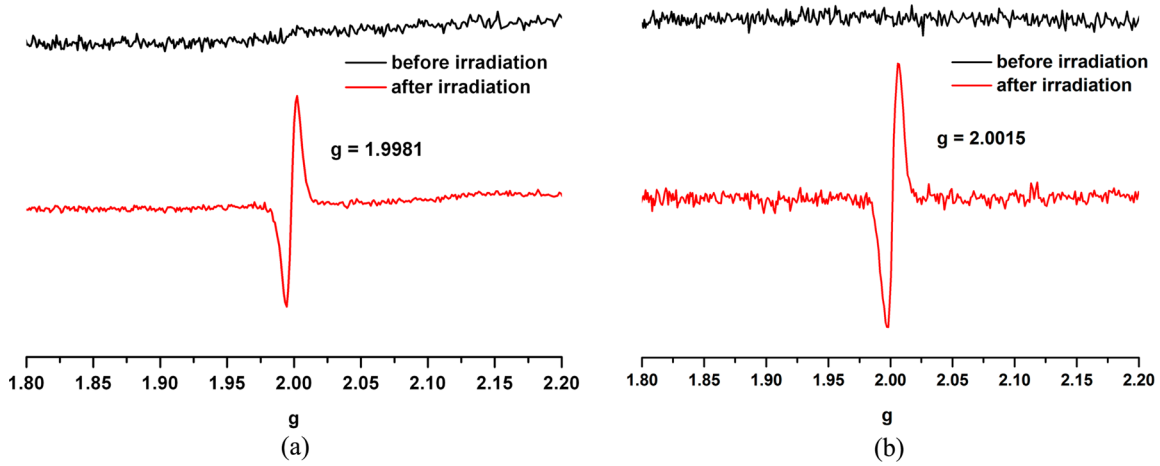

Figure 6. EPR spectra for (a) **1** and (b) **2** before and after irradiation in the solid state at room temperature.

Cg centroids are 3.584(4), 3.800(4) and 3.813(6) Å, and the dihedral angles of those are 1.74°, 4.99°, and 0.03°, respectively (see Table S3 in the Supporting Information). The shortest N···Cl distance in **2** belongs to N(301) ···Cl(3), with a value of 3.396(5) Å (see Figure 2b). The angle between the (N301···Cl3) direction and the plane of the pyridinium ring and that of Bi(1)−Cl(3)···N(301) are ∼89.96° and 112.71°, respectively. Ten (10) of the BzV^{2+} cations and one dibenzyl ether molecule surround each inorganic anion through electrostatic forces and stack along the *b*-axis to form a channel where the $[Bi_3Cl_{14}]^{5-}$ anions are encapsulated (see Figure S3b in the Supporting Information).

Photochromic Properties. As shown in Figure 5, compounds **1** and **2** exhibit interesting photochromic behaviors. Their colors changed clearly upon irradiation by sunlight or 365-nm UV light at room temperature in air. The pale yellow crystalline sample of **1** turns to pale green after illumination for 30 s and gives a new clear absorption band centered at 645 nm (Figure 5a). Its coloration tends to be saturated after illumination for 30 min. Compound **2** is highly photosensitive because a change from pale yellow to green can be detected by the eye upon exposure to UV light in air for 10 s, and its coloration was closely saturated after irradiation for 10 min (Figure 5b). The complete decoloration of the photoproduct of **2** required 9 h in the darknesss (see Figure S4 in the Supporting Information) or 10 min by annealing at 100 °C in air, while that of the photoproduct of **1** required 2 days in the darkness or 30 min by annealing at 100 °C. Meanwhile, the cyclical color change of **1** and **2** can be repeated up to at least 10 times by UV irradiation and heating, respectively, which implies their typical photochromic behavior.

Both **1** and **2** are EPR silent before irradiation or/and after heating but show single-line signals at g = 1.9981 and 2.0015, respectively, after irradiation (see Figure 6), which is similar to those found in MV^{2+} or other viologen compounds.[2,10,11] Therefore, their photochromism can be mainly assigned to the reversible interconversion between the monocation radical $[V]^{+\bullet}$ and the dication $[V]^{2+}$. This has been verified by the UV-vis data. A new and broad band at ∼645 nm for **1** and ∼630 nm for **2** gradually appears in the UV-vis reflectance spectra upon

dx.doi.org/10.1021/ic5002144 | Inorg. Chem. 2014, 53, 5538−5545

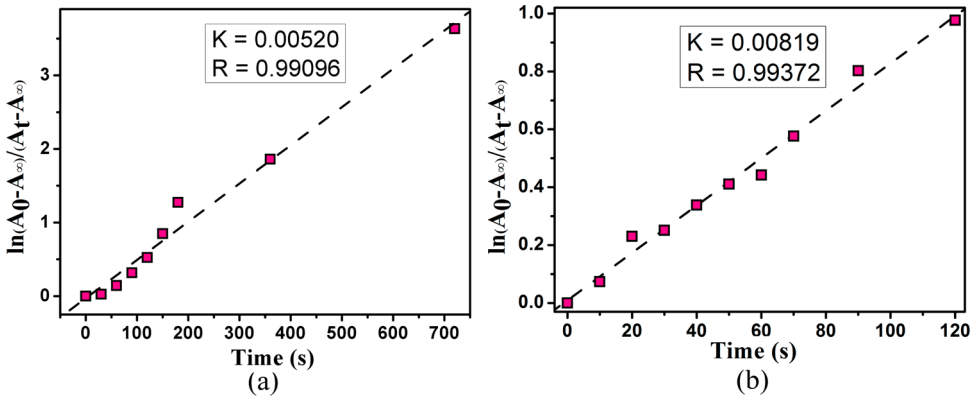

Figure 7. Photoinduced electron-transfer process kinetics of (a) **1** and (b) **2**.

irradiation with UV light. Such a change is very similar to those observed in other photochromic viologen compounds, and can be attributed to the production of the monocation radical in viologen.[12,13]

The kinetics of the photochemical reactions of **1** and **2** could be analyzed with eq (1):

$$\ln\left(\frac{A_0 - A_\infty}{A_t - A_\infty}\right) = kt \tag{1}$$

where k is the first-order rate constant, and A_0, A_t, and A_∞ are the absorbance at 645 nm for **1** and 630 nm for **2** at time zero, time t, and the photostationary stage, respectively.[14] Notably, the research of photochromic properties in metal-halide-based hybrid material is still relatively rare; the study of the kinetics of the photoinduced color change is even less. One reason is the reported compounds in this domain showed very slow photoresponse. For example, in $(MV)(Bi_2Cl_8)$[2a] and $(MV)_4(Bi_6Cl_{26})\cdot 2H_2O$,[2b] the coloration processes require several hours under the UV irradiation and the fade of color takes from several days to months. As shown in Figure 7, the linear fit of the data indicates the photoinduced electron-transfer process follows first-order reaction kinetics. The rate constants of **1** and **2** are 5.20×10^{-3} and 8.19×10^{-3} s^{-1}, respectively. It is clear that the photoresponsive rate of **2** is faster than that of **1**; moreover, all of them are faster than that of $(HBzV)_2[Bi_2Cl_{10}]$ ($k = 3.48 \times 10^{-3}$ s^{-1}).[2d]

As we know, the factors for the photoresponsive rate of photochromism include the distance of the pathway for charge transfer, the electron-accepting ability of V^{2+}, the electron-donating ability of the counterion of V^{2+}, and the stability of the species in the hybrid after donating or accepting electrons. A comparison of **1** and $(HBzV)_2[Bi_2Cl_{10}]$[2d] (Table 2) reveals that they contain the same electron-donating species, $[Bi_2Cl_{10}]^{4-}$; the electron-transfer pathway from an inorganic component to an organic component with the N···Cl distances of 3.332(4) Å in **1** are ~0.2 Å longer than that of $(HBzV)_2[Bi_2Cl_{10}]$ (3.106(3) Å); the DFT calculations show that the LUMO energies of BzV^{2+} in **1** and $HBzV^{2+}$ in $(HBzV)_2[Bi_2Cl_{10}]$ are −0.34664 and −0.37060 hartree (see Figure S5 in the Supporting Information), and the SOMO (singly occupied molecular orbital) energies of the monocation radical viologens ($BzV^{+\bullet}$ in **1**, $HBzV^{+\bullet}$ in $(HBzV)_2[Bi_2Cl_{10}]$), which originate from the viologen dication accepting one electron, are −0.26058 and −0.27204 hartree, respectively (see Figure S6 in the Supporting Information). Thus, the electron-accepting ability of $HBzV^{2+}$ is better than that of BzV^{2+}, and the stability of $HBzV^{+\bullet}$ is better than that of $BzV^{+\bullet}$. However, the photochemical reaction kinetics research shows that the photoresponsive rate of **1** is faster than that of $(HBzV)_2[Bi_2Cl_{10}]$. As we know, the $\pi\cdots\pi$ interactions among organic components may act as not only a powerful factor to stabilize the viologen monocation radicals but also the second electron-transfer pathway from π-conjugated substituents to viologen dications for a photochromic process.[2d] Comparing the crystal structures of **1** and $(HBzV)_2[Bi_2Cl_{10}]$ reveals that there exist only the edge-to-face $\pi\cdots\pi$ interactions (C−H···π interactions) in $(HBzV)_2[Bi_2Cl_{10}]$, while in **1**, there are not only the edge-to-face $\pi\cdots\pi$ interactions but also the face-to-face $\pi\cdots\pi$ interactions. Although the edge-to-face $\pi\cdots\pi$ distance in $(HBzV)_2[Bi_2Cl_{10}]$ (2.742 Å) is 0.189 Å shorter than that in **1** (2.931 Å), for the ability to stabilize the viologen monocation radical, the edge-to-face $\pi\cdots\pi$ interaction is weaker than the face-to-face $\pi\cdots\pi$ interaction.[15] Therefore, the face-to-face $\pi\cdots\pi$ interactions may be the crucial factor for the photoresponsive rate of **1** being faster than that of $(HBzV)_2[Bi_2Cl_{10}]$.

On the other hand, comparison of **1** and **2** (Table 2), they contain the same viologens as cations and the pathway of electron transfer from an inorganic component to an organic component with the N···Cl distances of 3.332(4) Å in **1** is slightly shorter than that of **2** (3.396(5) Å). However, the

Table 2. Comparison of Various Factors Affecting the Photochromism of 1, 2, and $(HBzV)_2[Bi_2Cl_{10}]$

possible factors to display photochromism	Value/Comment		
	1	**2**	$(HBzV)_2[Bi_2Cl_{10}]$
Charge Transfer			
N···Cl distance (Å)	3.332(4)	3.396(5)	3.106(3)
LUMO energy of V^{2+} (hartrees)	−0.34664	−0.34664	−0.37060
HOMO energy of anion (hartrees)	0.17593	0.23058	0.17593
edge-to-face $\pi\cdots\pi$ distance (Å)	2.931	2.951	2.742
face-to-face $\pi\cdots\pi$ distance (Å)	3.795(5)	3.584(4)	none
Stabilization of Viologen Monocation Radical			
counteranion	$[Bi_2Cl_{10}]^{4-}$	$[Bi_3Cl_{14}]^{5-}$	$[Bi_2Cl_{10}]^{4-}$
SOMO energy of $V^{+\bullet}$ (hartrees)	−0.26058	−0.26058	−0.27204
edge-to-face $\pi\cdots\pi$ distance (Å)	2.931	2.951	2.742
face-to-face $\pi\cdots\pi$ distance (Å)	3.795(5)	3.584(4)	none

dx.doi.org/10.1021/ic5002144 | Inorg. Chem. 2014, 53, 5538−5545

photoresponsive rate of **2** is faster than that of **1**, which can be explained from the following three aspects:

(i) Generally, the photoresponsive rate of viologen dication would diminish with the decrease of the size of the inorganic oligomer, because a smaller inorganic oligomer has a worse ability to stabilize the viologen radical monocation. The size of $[Bi_3Cl_{14}]^{5-}$ inorganic anion in **2** is obviously bigger than $[Bi_2Cl_{10}]^{4-}$ anion in **1**; thus, $[Bi_3Cl_{14}]^{5-}$ could stabilize the viologen radical monocation more easily than that of $[Bi_2Cl_{10}]^{4-}$.

(ii) Using DFT calculations, we evaluate the ability of the inorganic anion ($[Bi_{2n}Cl_{8n+2}]$, n = 0.5, 1, 1.5, 2, and 3) to donate electrons. The DFT calculations show that the HOMO energies of $[BiCl_6]^{3-}$, $[Bi_2Cl_{10}]^{4-}$, $[Bi_3Cl_{14}]^{5-}$, $[Bi_4Cl_{18}]^{6-}$, and $[Bi_6Cl_{26}]^{8-}$ are 0.14027, 0.17593, 0.23058, 0.27345, and 0.35655 hartree, respectively (see Table S4 in the Supporting Information). This indicates that the bigger inorganic anion has a better ability to donate electrons than that of the smaller inorganic anion in this series compound; in other words, the anion $[Bi_3Cl_{14}]^{5-}$ has a better ability to donate electrons than that of $[Bi_2Cl_{10}]^{4-}$.

(iii) Note that the edge-to-face $\pi\cdots\pi$ distance in **1** (2.931 Å) almost the same as that of **2** (2.951 Å), but the face-to-face $\pi\cdots\pi$ distance in **1** (3.795(5) Å) is 0.211 Å longer than that in **2** (3.584(4) Å), which means the electron can be transferred more easily in **2** than in **1**, resulting in the photoresponsive rate of **2** being faster than that of **1**.

CONCLUSIONS

In summary, we have prepared two new viologen metal halide hybrid compounds by an *in situ* solvothermal reaction, and compound **2** contains an unprecedented discrete trimer $[Bi_3Cl_{14}]^{5-}$ counterion. Furthermore, studies on the relationship between structure and photochromic behavior have confirmed that the size of an inorganic oligomer can influence the photoresponsive rate of a viologen dication, and the $\pi\cdots\pi$ interaction may act as not only a powerful factor to stabilize the viologen monocation radical but also the second electron-transfer pathway from a π-conjugated substituent to a viologen cation for a photochromic process. Our research offers a new method for the design and syntheses of new photochromic hybrids with excellent properties. Much more modification on the improved photochromic properties in this series compounds could be achieved by an organic strategy, for example, to introduce a bigger aromatic system instead of a benzene group into the viologen molecule. It is anticipated that the aforementioned methodology may be applied to prepare other viologen metal halide hybrid compounds with new topological structures and better photochromic performances.

ASSOCIATED CONTENT

Supporting Information

X-ray crystallographic data for **1** and **2** in CIF format. FT-IR spectra, PXRD patterns, selected bond lengths and bond angles, and hydrogen bond parameters for **1** and **2**, $\pi\cdots\pi$ interactions, and C−H$\cdots\pi$ interactions bond donor/acceptor schemes of **1** and **2**, as well as a DFT calculation. This material is available free of charge via the Internet at http://pubs.acs.org.

AUTHOR INFORMATION

Corresponding Author

*E-mail: gcguo@fjirsm.ac.cn.

Notes

The authors declare no competing financial interest.

ACKNOWLEDGMENTS

We gratefully acknowledge the financial support by the NSF of China (Nos. 21221001, 21271042, 21373225, 21101152), 973 program (No. 2013CB933203), and the NSF for Distinguished Young Scholars of Fujian Province (No. 2011J06006).

REFERENCES

(1) (a) Ford, P. C.; Vogler, A. *Acc. Chem. Res.* **1993**, *26*, 220. (b) Mitzi, D. B. *Prog. Inorg. Chem.* **1999**, *48*, 1. (c) Bujak, M.; Zaleski, J. *J. Solid State Chem.* **2004**, *177*, 3202. (d) Kulicka, B.; Kinzhybalo, V.; Jakubas, R.; Ciunik, Z.; Baran, J.; Medycki, W. *J. Phys.: Condens. Matter* **2006**, *18*, 5087. (e) Tershansy, M. A.; Goforth, A. M.; Gardinier, J. R.; Smith, M. D.; Peterson, L., Jr.; zur Loye, H.-C. *Solid State Sci.* **2007**, *9*, 410. (f) Bi, W.; Louvain, N.; Mercier, N.; Luc, J.; Rau, H.; Kajzar, F.; Sahraoui, B. *Adv. Mater.* **2008**, *20*, 1013. (g) Bi, W.; Mercier, N. *Chem. Commun.* **2008**, 5743. (h) Mercier, N.; Louvain, N.; Bi, W. *Cryst. Eng. Commun.* **2009**, *11*, 720. (i) Louvain, N.; Mercier, N.; Boucher, F. *Inorg. Chem.* **2009**, *48*, 879.

(2) (a) Xu, G.; Guo, G.-C.; Wang, M.-S.; Zhang, Z.-J.; Chen, W.-T.; Huang, J.-S. *Angew. Chem., Int. Ed.* **2007**, *46*, 3249. (b) Xu, G.; Guo, G.-C.; Guo, J.-S.; Guo, S.-P.; Jiang, X.-M.; Yang, C.; Wang, M.-S.; Zhang, Z.-J. *Dalton Trans.* **2010**, *39*, 8688. (c) Leblanc, N.; Bi, W.; Mercier, N.; Auban-Senzier, P.; Pasquier, C. *Inorg. Chem.* **2010**, *49*, 5824. (d) Lin, R.-G.; Xu, G.; Wang, M.-S.; Lu, G.; Li, P.-X.; Guo, G.-C. *Inorg. Chem.* **2013**, *52*, 1199. (e) Mercier, N. *Eur. J. Inorg. Chem.* **2013**, 19. (f) Toma, O.; Mercier, N.; Botta, C. *Eur. J. Inorg. Chem.* **2013**, 1113. (G) Wang, M.-S.; Xu, G.; Zhang, Z.-J.; Guo, G.-C. *Chem. Commun.* **2010**, *46*, 361.

(3) Blachnik, R.; Jaschinski, B.; Reuter, H.; Kastner, G. *Z. Kristallogr.* **1997**, *212*, 874.

(4) Leblanc, N.; Allain, M.; Mercier, N.; Sanguinet, L. *Cryst. Growth Des.* **2011**, *11*, 2064.

(5) Frisch, M. J.; Trucks, G. W.; Schlegel, H. B.; Scuseria, G. E.; Robb, M. A.; Cheeseman, J. R.; Montgomery, Jr., J. A.; Vreven, T.; Kudin, K. N.; Burant, J. C.; Millam, J. M.; Iyengar, S. S.; Tomasi, J.; Barone, V.; Mennucci, B.; Cossi, M.; Scalmani, G.; Rega, N.; Petersson, G. A.; Nakatsuji, H.; Hada, M.; Ehara, M.; Toyota, K.; Fukuda, R.; Hasegawa, J.; Ishida, M.; Nakajima, T.; Honda, Y.; Kitao, O.; Nakai, H.; Klene, M.; Li, X.; Knox, J. E.; Hratchian, H. P.; Cross, J. B.; Bakken, V.; Adamo, C.; Jaramillo, J.; Gomperts, R.; Stratmann, R. E.; Yazyev, O.; Austin, A. J.; Cammi, R.; Pomelli, C.; Ochterski, J. W.; Ayala, P. Y.; Morokuma, K.; Voth, G. A.; Salvador, P.; Dannenberg, J. J.; Zakrzewski, V. G.; Dapprich, S.; Daniels, A. D.; Strain, M. C.; Farkas, O.; Malick, D. K.; Rabuck, A. D.; Raghavachari, K.; Foresman, J. B.; Ortiz, J. V.; Cui, Q.; Baboul, A. G.; Clifford, S.; Cioslowski, J.; Stefanov, B. B.; Liu, G.; Liashenko, A.; Piskorz, P.; Komaromi, I.; Martin, R. L.; Fox, D. J.; Keith, T.; Al-Laham, M. A.; Peng, C. Y.; Nanayakkara, A.; Challacombe, M.; Gill, P. M. W.; Johnson, B.; Chen, W.; Wong, M. W.; Gonzalez, C.; and Pople, J. A. *Gaussian 03, Revision E.01*; Gaussian, Inc.: Wallingford, CT, 2004.

(6) *SHELXTL, Version 5 Reference Manual*; Siemens Energy & Automation, Inc.: Madison, WI, 1994.

(7) Ma, C. L.; Zhang, J. H.; Li, F.; Zhang, R. F. *Eur. J. Inorg. Chem.* **2004**, 2775.

(8) Chen, Y.; Yang, Z.; Guo, C.-X.; Ni, C.-Y.; Ren, Z.-G.; Li, H.-X.; Lang, J.-P. *Eur. J. Inorg. Chem.* **2010**, 5326.

(9) Chen, Y.; Wang, Z.-O.; Yang, Z.; Ren, Z.-G.; Lia, H.-X.; Lang, J.-P. *Dalton Trans.* **2010**, *39*, 9476.

(10) (a) Yoon, K. B.; Kochi, J. K. *J. Am. Chem. Soc.* **1988**, *110*, 6586–6588. (b) Xue, W. M.; Wang, Y.; Mak, T. C. W.; Che, C. M. *J. Chem.*

Soc., Dalton Trans. **1996**, 2827−2834. (c) Yoshikawa, H.; Nishikiori, S. *Chem. Lett.* **2000**, 142−143.
(11) (a) Bockmann, T. M.; Kochi, J. K. *J. Org. Chem.* **1990**, *55*, 4127−4135. (b) Vermoulen, L. A.; Thompson, M. E. *Nature* **1992**, *358*, 656−658.
(12) (a) Kamagawa, H.; Masui, T.; Amemiya, S. J. *Polym. Sci., Polym. Chem. Ed.* **1984**, *22*, 383. (b) Mao, Y.; Breen, N. E.; Thomas, J. K. *J. Phys. Chem.* **1995**, *99*, 9909. (c) Kamogawa, H.; Nanasawa, M. *Bull. Chem. Soc. Jpn.* **1993**, *66*, 2443.
(13) (a) *Applied Photochromic Polymer Systems*; McArdle, C. B., Ed.; Blackie: Glasgow, London, 1992. (b) Lee, D. K.; Kim, Y. I.; Kwan, Y. S.; Kang, Y. S.; Kevan, L. *J. Phys. Chem. B* **1997**, *101*, 5319.
(14) Sworakowski, J.; Janus, K.; Nešpurek, S. *Adv. Colloid Interface Sci.* **2005**, *116*, 97.
(15) (a) Nygaard, S.; Hansen, S. W.; Huffman, J. C.; Jensen, F.; Flood, A. H.; Jeppesen, J. O. *J. Am. Chem. Soc.* **2007**, *129*, 7354. (b) Manojkumar, T. K.; Choi, H. S.; Hong, B. H.; Tarakeshwar, P.; Kim, K. S. *J. Chem. Phys.* **2004**, *121*, 841.